Generation of GW-level radiation pulses from a VUV Self-Amplified Spontaneous Emission Free-Electron Laser operating in the femtosecond regime

V. Ayvazyan,[16] N. Baboi,[6] I. Bohnet,[1] R. Brinkmann,[3] M. Castellano,[7] P. Castro,[3] L. Catani,[9] S. Choroba,[3] M. Dohlus,[3] H.T. Edwards,[5] B. Faatz,[3] A.A. Fateev,[12] J. Feldhaus,[3] K. Flöttmann,[3] A. Gamp,[3] T. Garvey,[13] Ch. Gerth,[3] V. Gretchko,[10] B.Grigoryan,[16] U. Hahn,[3] C. Hessler,[3] K. Honkavaara,[3] M. Hüning,[15] R. Ischebek,[3] M. Jablonka,[1] T. Kamps,[4] M. Körfer,[3] M. Krassilnikov,[2] J. Krzywinski,[11] M. Liepe,[6] A. Liero,[15] T. Limberg,[3] H. Loos,[3] C. Magne,[1] J. Menzel,[15] P. Michelato,[8] M. Minty,[3] A. Mosnier,[1] U.-C. Müller,[3] D. Nölle,[3] A. Novokhatski,[2] C. Pagani,[8] F. Peters,[3] J. Pflüger,[3] P. Piot,[3] L. Plucinski,[6] K. Rehlich,[3] I. Reyzl,[3] A. Richter,[2] J. Rossbach,[3] E.L. Saldin,[3] W. Sandner,[14] H. Schlarb,[6] G. Schmidt,[3] P. Schmüser,[6] J.R. Schneider,[3] E.A. Schneidmiller,[3] H.-J. Schreiber,[4] S. Schreiber,[3] D. Sertore,[8] S. Setzer,[2] S. Simrock,[3] R. Sobierajski,[3] B. Sonntag,[6] B. Steeg,[3] F. Stephan,[4] K.P. Sytchev,[12] K. Tiedtke,[3] M. Tonutti,[15] R. Treusch,[3] D. Trines,[3] D. Türke,[3] V. Verzilov,[7] R. Wanzenberg,[3] T. Weiland,[2] H. Weise,[3] M. Wendt,[3] I. Will,[14] S. Wolff,[3] K. Wittenburg,[3] M.V. Yurkov,[12] and K. Zapfe[3]

[1] *CEA Saclay, 91191 Gif s/Yvette, France*
[2] *Darmstadt University of Technology, FB18 - Fachgebiet TEMF, Schlossgartenstr. 8, 64289 Darmstadt, Germany*
[3] *Deutsches Elektronen-Synchrotron DESY, Notkestrasse 85, 22603 Hamburg, Germany*
[4] *Deutsches Elektronen-Synchrotron DESY, Platanenallee 6, 15738 Zeuthen, Germany*
[5] *Fermi National Accelerator Laboratory, MS 306, P.O. Box 500, Batavia, IL 60510 USA*
[6] *Hamburg University, Inst. f. Experimentalphysik, Notkestrasse 85, 20603 Hamburg, Germany*
[7] *INFN-LNF, via E. Fermi 40, 00044 Frascati, Italy*
[8] *INFN Milano - LASA, via Fratelli Cervi 201, 20090 Segrate (MI), Italy*
[9] *INFN-Roma2, via della Ricerca Scientifica 1, 00100 Roma, Italy*
[10] *Institute for Nuclear Research of RAS, 117312 Moscow, 60th October Anniversary prospect 7A, Russia*
[11] *Institute of Physics, Polish Academy of Sciences, al. Lotnikow, 32/46, 02-668 Warsaw, Poland*
[12] *Joint Institute for Nuclear Research, 141980 Dubna, Moscow Region, Russia*
[13] *Laboratoire de l'Accélérateur Linéaire, IN2P3-CNRS, Université de Paris-Sud, B.P. 34, F-91898 Orsay, France*
[14] *Max-Born-Institute, Max-Born-Str. 2a, 12489 Berlin, Germany*
[15] *RWTH Aachen-Physikzentrum, Phys. Inst. IIIa, Sommerfeldstr. 26-28, 52056 Aachen, Germany*
[16] *Yerevan Physics Institute, 2 Alikhanyan Brothers str., 375036 Yerevan, Armenia*

(Dated: November 2, 2001)

We present experimental results of Self-Amplified Spontaneous Emission (SASE) free-electron laser (FEL) operating in the mode of super-short pulse duration (30–100 fs FWHM) with the peak radiation power at a GW level and a full transverse coherence. During the experiment the radiation wavelength was tuned in the range of 95-105 nm.

PACS numbers: 41.60.Cr,29.17.+w,29.27.-a,Fh,41.75.Lx,29.25.Bx,52.75.Va

The experimental results presented in this paper have been achieved at the TESLA Test Facility (TTF) Free-Electron Laser at the Deutsches Elektronen-Synchrotron DESY [1–3]. In the VUV free electron laser at DESY the radiation is produced by the electron beam during a single-pass trough the undulator [4, 5]. The amplification process starts from shot noise in the electron beam. During the amplification process powerful, coherent radiation is produced having a narrow band near the resonance wavelength. In the high-gain linear regime the radiation power $P(z)$ grows exponentially with the distance z along the undulator [6–8]:

$$P(z) = P_0 \exp(z/L_g) \, ,$$

where L_g is the power gain length. Since first lasing of the SASE FEL at DESY [9] its performance has been gradually improved. The radiation wavelength is continuously tunable in a wide range from 80 to 180 nm [10]. In this paper we report on achieving saturation with the peak output radiation power at a GW level. The energy in the radiation pulse is 30-100 μJ, the pulse duration is 30-100 fs. The peak brilliance is 10^{29} phot./sec/mrad^2/mm^2/(0.1% BW.), nine orders of magnitude higher than at state-of-art 3rd generation synchrotron radiation sources. Degeneracy parameter (number of photons per mode) is about 10^{14} and thus has the same order of magnitude as that quantum lasers operating in visible. During experiment TTF FEL operated at the repetition rate up to 60 pulses per second with the average radiation power up to 5 mW. Even with such a low repetition rate the average brilliance is 10^{18} phot./sec/mrad^2/mm^2/(0.1% BW.), an order of magnitude above the corresponding value for 3rd gener-

TABLE I: Main parameters of the TESLA Test Facility for FEL experiments (TTF FEL, phase 1)

beam energy	240 – 250 MeV
bunch charge	2.7-3.3 nC
charge in radiative part of the beam	0.1-0.2 nC
duration of radiative part of the beam	50-150 fs
peak current	1 – 1.5 kA
rms energy spread	100 – 200 keV
rms normalized emittance (slice)	4 – 7 π mrad mm
bunch spacing	0.44 / 1 μs
number of bunches in a train	up to 60
repetition rate	1 Hz
undulator period	27.3 mm
undulator peak field	0.47 T
Averaged beta-function	1.2 m
effective undulator length	13.5 m
radiation wavelength	95-105 nm
energy in the radiation pulse	30 – 100 μJ
radiation pulse duration	30-100 fs
radiation peak power	1 GW
radiation average power up to	5 mW
spectrum width (FWHM)	1%
radiation spot size (FWHM)	250 μm
radiation angular divergence (FWHM)	260 μrad

ation SR sources.

A detailed description of the experimental facility has been presented in [9]. The main parameters for FEL operation are compiled in Table I. The TTF FEL consists of a driving accelerator producing bunches with an energy up to 300 MeV, and a 14.1 m long undulator [11]. The injector consists of a laser-driven rf gun [12–14], followed by a capture cavity, boosting the energy to 16 MeV. The main accelerator consists of two superconducting accelerator modules [15] separated by a magnetic bunch compressor [16]. At 3 nC, the longitudinal charge density upstream of the main linac is expected to follow a Gaussian distribution with 4 mm rms length. As a consequence of the long bunch compared to the rf-wave length (23 cm), the bunch longitudinal phase space accumulates an rf-induced curvature during its acceleration in the first accelerating module. This distortion results, downstream of the bunch compressor, in a non-Gaussian distribution with a local charge concentration. Simulation results of the described experimental situation are presented in Fig. 1. This numerical result is consistent with estimated peak current of 1 – 1.5 kA inferred from the measurement of the FEL radiation properties.

Characterization of the FEL radiation has been performed by means of measurements of the radiation energy, spectral characteristics, angular distribution, and statistical properties.

Figure 2 presents the average energy in the radiation pulse versus undulator length. The interaction length has been changed by means of switching on electromagnetic correctors installed inside the undulator. The value of the orbit kick provided by a corrector is sufficient to

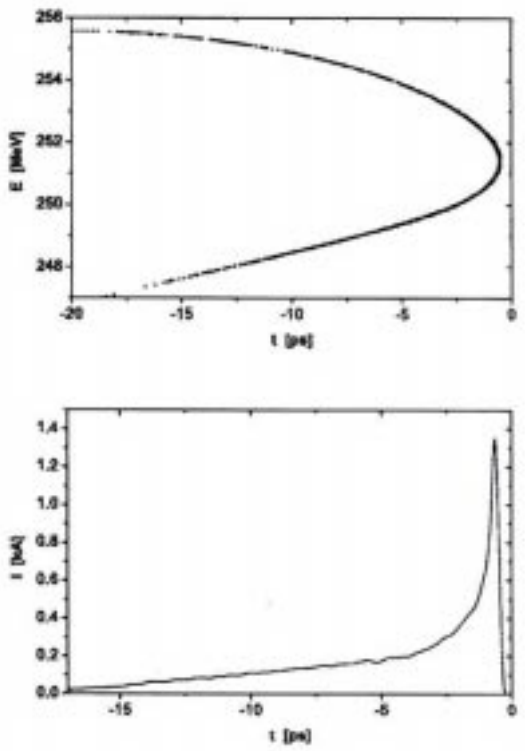

FIG. 1: Simulations of the longitudinal phase space distribution of the electrons at the undulator entrance (upper plot). Lower plot presents distribution of the current along the bunch. Head of the bunch is on the right side. Here bunch charge is 3 nC.

stop FEL amplification process downstream the corrector. The radiation energy has been measured by means of an MCP-based detector of 10 mm diameter installed 12 m downstream the undulator [17]. When the FEL interaction is suppressed along the whole undulator length, the detector shows the level of spontaneous emission of about 2.5 nJ collected from the full undulator length. Then FEL interaction was switched on gradually along the undulator and the energy in the radiation pulse reached the value between 30 and 100 μJ depending on the accelerator tuning. Independent measurements of the radiation energy at saturation were taken by thermopile [19]. Results of both measurements agree well. All the results presented in this paper correspond to the tuning for 50 μJ radiation pulse energy. Analysis of the exponential part of the gain curve presented in Fig. 2 gives us the value for the power gain length of about $L_g = 67 \pm 5$ cm.

Each point in Fig. 2 was averaged over 100 shots. The energy in the radiation pulse fluctuates from shot to shot. The plot for standard deviation σ, is presented in Fig. 3. At the initial stage fluctuations are defined mainly by the fluctuations of the charge in the electron bunch. When

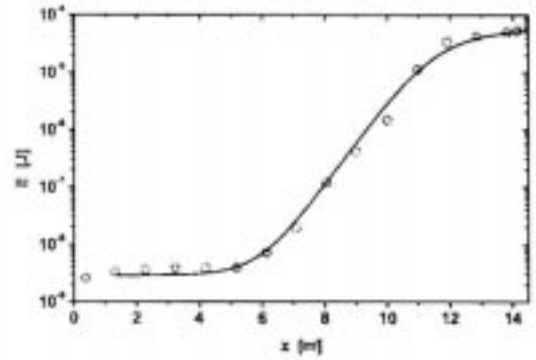

FIG. 2: Average energy in the radiation pulse versus undulator length. Circles – experimental results. Solid curve – numerical simulations with code FAST.

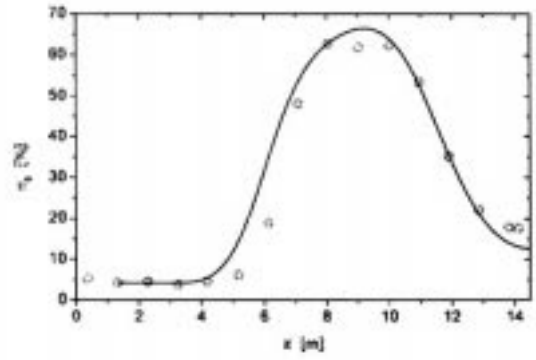

FIG. 3: Fluctuations of energy in the radiation pulse versus undulator length. Circles – experimental results. Solid curve – numerical simulations with code FAST.

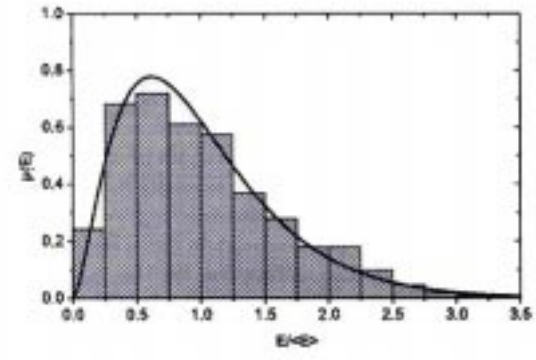

FIG. 4: Measured probability distribution of the energy in the radiation pulse at the undulator length of 9 m. Solid line represents gamma distribution with $M = 2.5$.

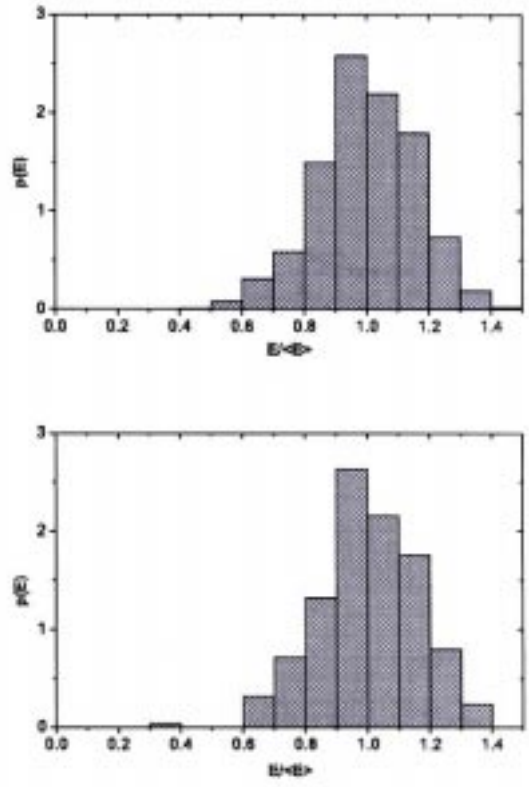

FIG. 5: Probability distribution of the energy in the radiation pulse at the undulator length of 14 m. Upper plot – experimental results. Lower plot – simulations with code FAST.

the FEL amplification process takes place, fluctuations of the radiation energy are mainly given by the fundamental statistical fluctuations of the SASE FEL radiation [18]. A sharp drop of the fluctuations in the last part of the undulator is a clear physical confirmation of the saturation process. When the FEL amplifier operates in the high-gain linear regime, the value of parameter $M = 1/\sigma^2$ gives the number of spikes (wavepackets) in the radiation pulse. In the case under study it is about $M \simeq 2.5$. This allows us to estimate the radiation pulse length as $\tau_{\rm rad} \simeq M L_c/c$. The cooperation length is about $L_c \simeq 2\lambda L_g/\lambda_u \simeq 5\mu$m. As a result, we obtain an estimation for the radiation pulse duration of about 50 fs.

Figure 4 shows the probability distribution of the energy in the radiation pulse measured at the undulator length of 9 meters corresponding to the high gain linear mode of operation. It is seen that the probability distribution is the gamma distribution. This experimental result is in good agreement with the prediction that the radiation from a SASE FEL operating in the linear regime possesses features of completely chaotic polarized light [18]. When amplification enters the nonlinear stage,

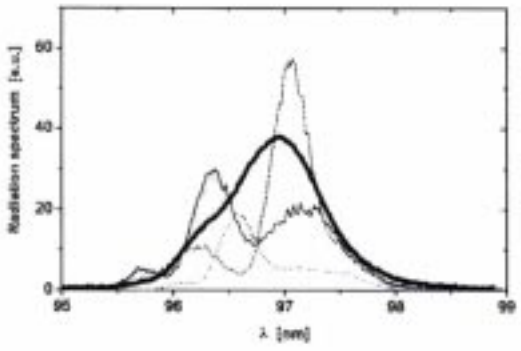

FIG. 6: Spectrum of the radiation (experimental results). Thin curves are single-shot spectra. Bold curve represents averaged spectrum.

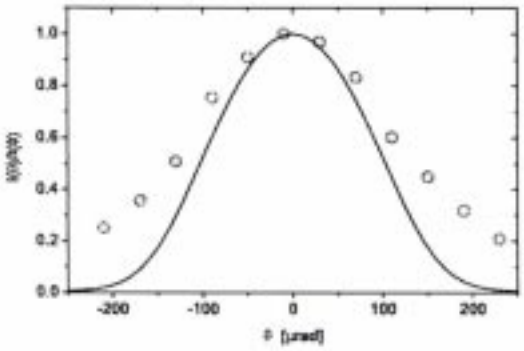

FIG. 7: Angular distribution of the radiation intensity at the undulator exit. Circles – experimental results. Solid curve – numerical simulations with code FAST.

this property is no longer valid, as it is illustrated with Fig. 5.

Results of spectral measurements are presented in Fig. 6. Single-shot spectra were taken with a monochromator of 0.2 nm resolution [19]. Images from the monochromator were detected by an intensified CCD camera. The bold curve in this plot presents spectrum averaged over 100 shots. Figure 7 shows the angular divergence of the FEL radiation. Measurements were performed by means of scanning the radiation beam with a 0.5 mm aperture installed in front of the radiation detector.

Information presented in Figs. 2-6 is sufficient to perform preliminary estimation of the parameter space. Using the value of the FWHM spectrum width, $(\Delta\omega)_{\rm FWHM}$, we can estimate the radiation pulse length as [8] $\tau_{\rm rad} \simeq 2M\sqrt{\pi}/(\Delta\omega)_{\rm FWHM} \simeq 50$ fs. Analysis of the measured single-shot spectra shows that typical width of the spike in the spectral domain, $\Delta\omega \simeq 1/\tau_{\rm rad}$, is in good qualitative agreement with estimated value of the pulse duration. It is well known that the FWHM spectrum width, $(\Delta\omega)_{\rm FWHM}$, corresponds approximately to 2ρ [8], where ρ is FEL parameter [20]. Analysis of the averaged spectrum (see Fig. 6) gives an estimation for the FEL parameter $\rho \simeq 4 \times 10^{-3}$. Remembering that the estimation for the radiation pulse energy is given by $E_{\rm rad} \simeq \rho I \mathcal{E} \tau_{\rm rad}$ [8], we come to the estimation for the value of the peak current $I \simeq 1$ kA. This estimation for the duration of the radiative part of the electron beam and for the value of peak current is in good agreement with parameters for the electron beam discussed above.

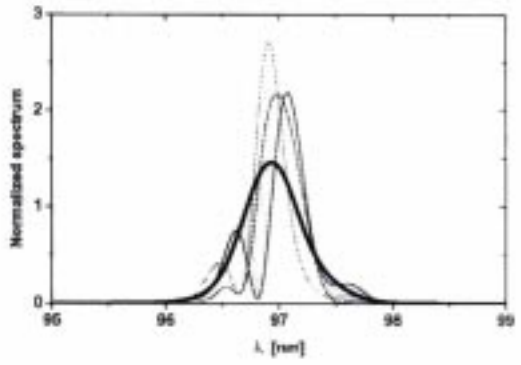

FIG. 8: Spectrum of the radiation (simulation with code FAST). Thin curves are single-shot spectra. Bold curve represents averaged spectrum.

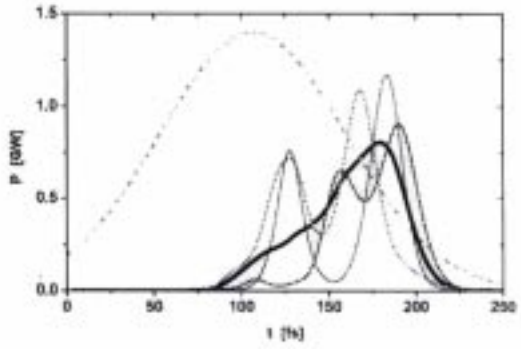

FIG. 9: Temporal structure of the radiation pulse calculated with code FAST. Thin curves are single-shot pulses. Bold curve represents averaged temporal structure. FWHM pulse duration is 50 fs. Dotted line denotes longitudinal profile of the head of the electron bunch approximated by Gaussian (see Fig. 1).

More deep analysis of the FEL operation can be done only with numerical simulation codes. Calculations have been performed with three-dimensional, time-dependent

FEL code FAST [21]. Starting point is the choice of the model for the electron bunch. Analysis of simulation results on the electron bunch formation (see Fig. 1) show that only head of the bunch is capable to generate FEL radiation. In the FEL simulations this part of the bunch (i.e. radiative part) was approximated with gaussian longitudinal current profile. The results of these simulations show that the most probable parameters for the radiative part of the electron beam are $\sigma_z \simeq 15\mu$m, $I \simeq 1.3$ kA, rms energy spread about 100 keV, rms normalized emittance $\epsilon_n \simeq 6\pi$ mm-mrad. Simulation results (calculated over 250 statistically independent runs) are presented in the plots for comparison with experimental results. One can see good quantitative agreement. The only visible difference refers to the averaged spectrum (see Figs. 6 and 8). The measured spectrum width of 1% FWHM is wider than the simulated one (0.7%). The reason for this could be shot-to-shot energy jitter of the electron beam.

Good agreement between experimental and simulation results allows us to specify parameters of the FEL which can not be measured directly, but recalculated from experimental data. First of all this refers to temporal structure of the radiation pulse (see Fig. 9). It is seen that a set of experimental observations presented above should correspond to the peak power close to one GW at 50 fs pulse duration (FWHM). Another important characteristic is the distribution of the radiation intensity at the undulator exit. Spot size of the radiation is approximately equal to the spot size of the electron beam. Simulations give the value of the FWHM spot size of the radiation 250 μm. Taking into account the measured angular divergence of about 260 μrad FWHM, we conclude that within accuracy of measurements output radiation has full transverse coherence.

[1] W. Brefeld, et al., Nucl. Instr. and Meth. **A393,** 119-124 (1997)

[2] T. Åberg, et al., A VUV FEL at the TESLA Test Facility at DESY, Conceptual Design Report, DESY Print TESLA-FEL 95-03 (1995)

[3] J. Rossbach, Nucl. Instr. and Meth. **A 375,** 269 (1996)

[4] A.M. Kondratenko, E.L. Saldin, Part. Accelerators **10,** 207 (1980)

[5] R. Bonifacio, C. Pellegrini, L.M. Narducci, Opt. Commun. **50,** 373 (1984)

[6] K.J. Kim, Phys. Rev. Lett. **57,** 1871 (1986)

[7] S. Krinsky,L.H. Yu, Phys. Rev. **A35,** 3406 (1987)

[8] E.L. Saldin, E.A. Schneidmiller, M.V. Yurkov, "The Physics of Free Electron Lasers" (Springer-Verlag, Berlin, 1999).

[9] J. Andruszkow et al., Phys. Rev. Lett. **85**(2000)3825.

[10] J. Rossbach, Proceedings of EPAC2000 Conference (Vienna, Austria, June 2000), p.88.

[11] J. Pflüger, Nucl. Instr. and Meth. **A445,** 366 (2000)

[12] J.-P. Carneiro, et al., Proc. 1999 Part. Acc. Conf., New York, 2027-2029 (1999)

[13] P. Michelato, et al., Nucl. Instr. and Meth. **A445,** 422 (2000)

[14] I. Will, S. Schreiber, A. Liero, W. Sandner, Nucl. Instr. and Meth. **A445,** 427 (2000)

[15] H. Weise, Proc. 1998 Linac Conf. Chicago, 674-678 (1998)

[16] T. Limberg et al., Nucl. Instr. and Meth. **A375**(1996)322.

[17] B. Faatz et al., DESY Print TESLA-FEL 2001-09 (Contributions to the FEL2001 Conference, August 20-24, 2001, Darmstadt, Germany), pp. 62-67.

[18] E.L. Saldin, E.A. Schneidmiller and M.V. Yurkov, Opt. Commun. **148**(1998)383.

[19] R. Treusch et al., Nucl. Instrum. and Methods **A467-468** (Part 1) (2001)30.

[20] R. Bonifacio, et al., Phys. Rev. Lett. **73,** 70 (1994)

[21] E.L. Saldin, E.A. Schneidmiller and M.V. Yurkov, Nucl. Instrum. and Methods **A429**(1999)233.